

Computational Investigation of Base Drag Reduction Techniques in a Typical Sounding Rocket

Abhilash B K¹, Anasooya Sen², Mohammed Nafas³, Varun V Anil⁴, Sanjoy Kumar Saha⁵, Aswathi Krishna⁶

^{1,2,3,4}Dept. of Aeronautical Engineering, ILM College of Engineering & Technology, Ernakulam, Kerala, India

^{5,6}Scientist/Engineer, Vikram Sarabhai Space Centre (VSSC), Thiruvananthapuram, Kerala, India

Abstract: - Aerospace vehicles undergo reduction in flight performance due to the effect of drag. When a bluff body travels, a low-pressure region is formed in the rear end of the body due to the flow separation at the blunt base. This phenomenon tends to cause the high-pressure air from the surrounding to flow into the region of low-pressure region forming wake, which create drag. Drag in the base region is one of the major contributors of aerodynamic drag, especially in the absence of jet at the base. For this reason, the minimization of base drag has been an important issue to date and considerable effort has been made to find suitable technique to reduce base drag. Since base drag is a type of pressure drag, it can be decreased in magnitude by using active and passive flow modification devices. In this study different modified base and fin regions are used in order to achieve a reduction in base drag. The analysis was done by computational means. The behaviors at different speed regimes are also studied, at Mach 0.8, 0.9, 1.05 and 1.20. Considerable reduction in drag coefficients is obtained by boat-tailing the base region. It turns out to be evident that implementation of base geometry modification contributes in total drag reduction.

Key Words: Base drag reduction, pressure drag, boat tailing, boundary layer, aft body modification, base cavity, tapered fin

1. INTRODUCTION

Sounding rockets are one or two stage solid propellant rockets used for probing the upper atmospheric regions and for space research. Sounding rockets take their name from the nautical term "to sound", which means to take measurements. They also serve as easily affordable platforms to test or prove prototypes of new components or subsystems intended for use in launch vehicles and satellites.

Aerodynamic bodies such as missiles, projectiles and rockets, generally, undergo a reduction in their desired flight performance due to the effect of drag. For these kinds of flight bodies, especially, the drag in the base region has a significant contribution to total drag. At transonic speeds, for example, base drag constitutes a major portion of up to 50% of the total drag^[1] for typical projectiles. Base drag should, therefore, be considered separately from other pressure-drag components. For this reason, the minimization of base drag has been an important issue to date, and considerable effort has been made to find suitable techniques for obtaining low base-drag shell design. Base drag reduction can be achieved by after body boat tailing, base bleed or base burning, some vortex suppression devices and their combinations^{[2][3][4]}. Basically, such active or passive flow control techniques^[2], manipulate or alter the near-wake flow-field for an increase in base pressure and consequently reduce base drag.

1.1 Aerodynamics of sounding rockets

Aerodynamic forces affect a body immersed in a fluid medium. These forces are due to the relative motion between the body and the fluid. When two solid objects interact in a mechanical process, forces are transmitted at the point of interaction. In contrast, aerodynamic forces on a solid body immersed in a fluid act on every point on the surface of the body. These forces are due to pressure distribution over the surface of the body and shear stresses arising from fluid viscosity. The forces acting on the rocket are the thrust force, weight, drag and lift.

Drag force is an aerodynamic force which is generated by the interaction of solid body with fluid and is not generated by a force field. The types of drag acting on a rocket body are skin friction drag, pressure/form drag and wave drag.

Skin friction drag: Skin friction^[5] arises from the friction of the fluid against the surface of the object that is moving through it. Skin friction arises from the interaction between the fluid and the skin of the body. This depends on type of flow (i.e. laminar or turbulent).

Pressure drag or form drag: Pressure drag arises because of the form of the object. The general size and shape of the body is the most important factor in form drag. Bodies with a larger apparent cross section will have a higher drag than thinner

bodies. Sleek designs, or designs that are streamlined or that change cross-sectional area gradually are also critical for achieving minimum form drag. Elimination of vortices in the wake reduces pressure drag.

Wave drag: Wave drag is caused by the formation of shock waves around the aircraft which radiate away a considerable amount of energy producing enhanced drag. The effect is mainly seen at transonic and supersonic areas, but the effect may arise at lower speed at the areas where local Mach number slips to supersonic regime.

1.2 BASE DRAG

It is the drag generated in an object moving through a fluid from the shape of its rear end. The Factors affecting base drag

Base drag is influenced by a variety of flow and geometrical parameters. With turbulent boundary layer ahead of the base, and in the absence of jet flow, the major factors include:

- After body shape (boat-tail or flare angle, fore body diameter, after body length)
- Base diameter
- Mach number in the free stream, just ahead of the base.
- Boundary layer momentum thickness ahead of the base
- Parameters characterising the base drag reduction device

In order to achieve base drag reduction which is a type of form drag several techniques including geometry alteration is done. The different techniques used are

- Aft body shape alteration
- Fin design alteration
- Passive control methods
- Active control devices

1.2.1 After body modifications

- **Boat tailing**

In boat tailing, the base of the body is getting narrowed. Since the base of the body is narrowed, the flow separation at the aft end of the vehicle is delayed, reducing the size of the wake formed. Hence the velocity in the base area will be reduced. Then according to Bernoulli's principle, the pressure will be increased in the base area. The increase in base area pressure will reduce the base drag.

- **Base bleed**

Base bleeding is a vital technique used for base drag reduction. In base bleeding small amount of gas is injected into the flow field behind the base projectile. This will split the ordinary large recirculation zone into two parts, one symmetry to axis and the other formed right behind the base corner [2]. Without base bleeding effect a large and strong recirculation flow is observed, and this will decrease the base pressure and increase the base drag. With base bleeding the strength of recirculation zone is reduced and will increase the base pressure and this will contribute in the decrement of base drag.

- **Base cavity**

Base cavities (hollow extensions mounted behind the rear end of a bluff body) are known to reduce substantially the aerodynamic drag of two-dimensional bodies [6]. When the flow separates and a large vortex is formed behind the bare airfoil, a cavity can capture that flow and stabilize it, therefore allowing a less turbulent flow to form, creating more base pressure [1]. It was Morel [2] who demonstrated the potential benefits of axisymmetric base flow at low speed the drag.

- **Boundary layer thickness**

Another method of reducing base drag is by increasing the boundary layer thickness. The flow coming from the aft body accelerates the fluid in the base area and hence base pressure is reduced thereby increasing the base drag [7]. By increasing the boundary layer thickness in aft body, the flow separation occurs at the aft body, hence the flow which accelerates the fluid in the base will be reduced thereby increasing the base pressure. Hence base drag gets reduced.

- **Multi-step after bodies**

A multi-step after body generally consists of many (backward facing) annular steps ahead of the base; a toroidal vortex results from the separation and reattachment at each step ^{[2] [3] [4]}. Such a configuration will have a lower base area (like a boat-tailed base), and a reduction in base drag relative to the unmodified blunt base can be realized if the step geometry is properly selected. The trapped vortex in each step also contributes in the total base drag reduction

2. SOFTWARE USED

In this project, CATIA V5 software is used for designing the various model used for analysis. PARAS 3D (Parallel Aerodynamic Simulator) & ANSYS software are used for CFD simulation.

2.1 CATIA

CATIA software is a multi-platform software suite for computer-aided design, computer-aided manufacturing, computer-aided engineering, PLM and 3D, developed by the French company Dassault Systems. CATIA supports multiple stages of product development (CAx), including conceptualization, design (CAD), engineering (CAE) and manufacturing (CAM). CATIA facilitates collaborative engineering across disciplines around its 3D EXPERIENCE platform, including surfacing & shape design, electrical, fluid and electronic systems design, mechanical engineering and systems engineering. All the CAD models are prepared using CATIA V5.

2.2. PARAS

PARAS (Parallel Aerodynamic Simulator) 3D Software is an inhouse, general purpose, flow analysis and simulation software of ISRO. It has been successfully applied to large scale simulation problems such as flow over a complete multi body launch vehicle configuration with strap on boosters, flow over a complete aircraft with wing, fuselage, stores etc. The code has been thoroughly validated by applying to a number of flow simulation problems where the results are known from either wind tunnel experiments or from other numerical simulations using established codes. It has been successfully applied to a number of complex practical problems in the aerospace domain.

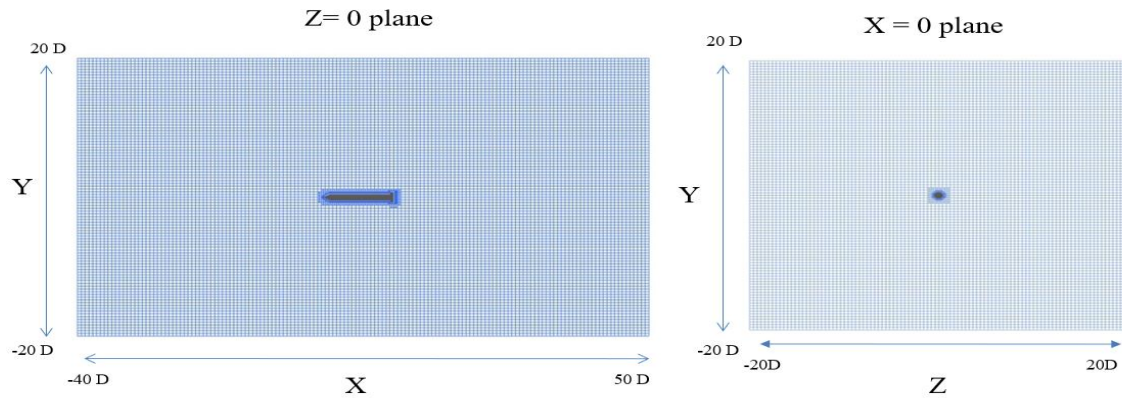
2.3 ANSYS

ANSYS software contains the broad, physical modeling capabilities needed to model flow, turbulence, heat transfer and reactions for industrial applications. The software spans an expansive range, including special models, with capabilities to model in-cylinder combustion, aero-acoustics, turbo machinery and multiphase systems. Fluent also offers highly scalable, high-performance computing (HPC) to help solve complex, large-model computational fluid dynamics (CFD) simulations quickly and cost-effectively. More defined flow characteristic near the body surface is obtained in ANSYS, which help in analysis of boundary layer formation. There are different versions of the software available in this study ANSYS 2019 R3 ACADEMIC is used.

3. SIMULATION PARAMETERS

3.1 Grid And Domain

The details of the domain used for PARAS are shown in Fig 1. PARAS 3D uses an inbuilt cartesian grid generation for meshing. The domain is divided in 150 cells along the length and 100 cells along the lateral directions. Each cell is further sub divided multiple times till the geometry of the body is accurately captured. All the criteria for gridding are set similar for all other models used in this study.



*D is the base diameter

Fig. 1 Domain with grid

3.2 Simulation Condition

In the study compressible Navier Stokes equation is solved on the grid with courant number as 0.1. For each case, flow simulation is carried out for four different transonic Mach numbers as base drag peaks in this regime. The Mach numbers considered are 0.80, 0.90, 1.05, and 1.20. Domain of simulation (Table 1) and simulation conditions are set similar for all cases with exception in boundary condition, and free stream conditions. Standard values for pressure and density are taken for each Mach number, corresponding to free stream conditions of NAL 1.2 m wind tunnel. Subsonic and supersonic Mach numbers are simulated with different boundary conditions, that is, pressure for subsonic and shift for supersonic. The angle of attack α is taken as 4 degrees for all cases and Mach numbers. Details about the free stream parameters used for simulation are given in Table 2.

Table 1 Domain used for the simulations

	MIN (m)	MAX (m)
X (m)	-20	25
Y (m)	-10	10
Z (m)	-10	10

All the aerodynamic coefficients are reported with body diameter (0.5 m) as the reference length, and the corresponding cross-sectional area (0.19635 m²) as the reference area. All the moment coefficients are computed with origin (nose tip) as the reference point.

Table 2 Free stream properties used for all cases stream properties used for all cases

Mach	α (degree)	β (degree)	ρ (kg/m ³)	P (N/m ²)	Gamma (γ)	Mol. mass (kg/mol)
0.80	4	0	1.496	113061.6	1.4	0.02897
0.90	4	0	1.389	101893.3	1.4	0.02897
1.05	4	0	1.229	85830.3	1.4	0.02897
1.20	4	0	1.074	71077.1	1.4	0.02897

4. BODY CONFIGURATIONS AND FINS USED

In the study the effect of base geometry and fin geometry modification are considered. A total of 5 different rocket configurations have been studied using PARAS. To have a better understanding of the effect of fin geometry modification, separate CFD simulation has been carried out over 5 different isolated fin configurations using PARAS and ANSYS. These designs are analysed under different conditions (Table 2) to obtain the result.

Body Configuration Considered:

4.1 Basic Reference Model

A typical sounding rocket configuration is taken as basic reference model. The dimensions taken for the reference model is given in Table 3. All other results are compared with the results from this basic configuration.

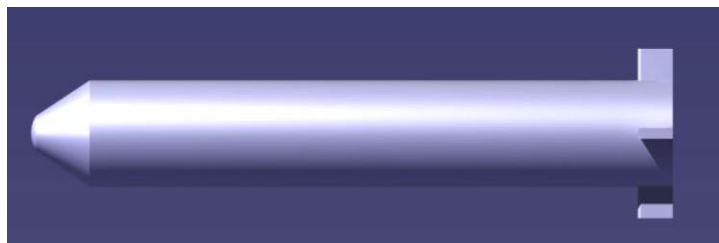


Fig. 2 3D model of basic reference mode

Table 3 Dimensions of reference model

Total length	5501.167mm
Nose cone radius	100mm
Body diameter	500mm
Nose cone semi vertex angle	20 degree
Fin root chord	300mm
Fin semi span	150mm
Fin thickness	50mm
Fin tip radius	2mm
Fin tip angle	45 degree

4.2 Boat Tailing

Boat tailing is a type base drag reduction technique in which cross-sectional area of the base is gradually reduced. For this study, boat tailing is started at 15% of total length from the base, keeping other dimensions same as the reference model. The boat tailing angle is 6.9 degree.

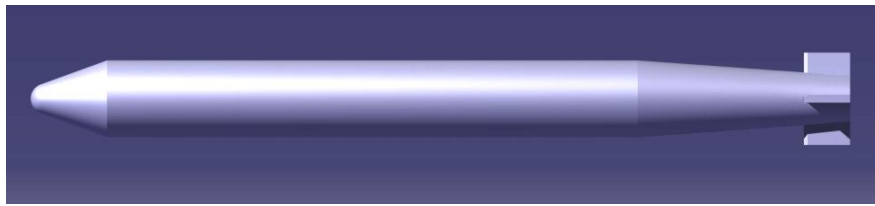


Fig. 3 Configuration with boat tailing at the base

4.3 Base Cavity

Base cavity is another method used for base drag reduction. Here, the base cavity of diameter 300mm with a pocket length of 200mm is chosen. The only change with respect to the reference model is the cavity at the base. The remaining dimensions and geometry are retained same as the reference model.

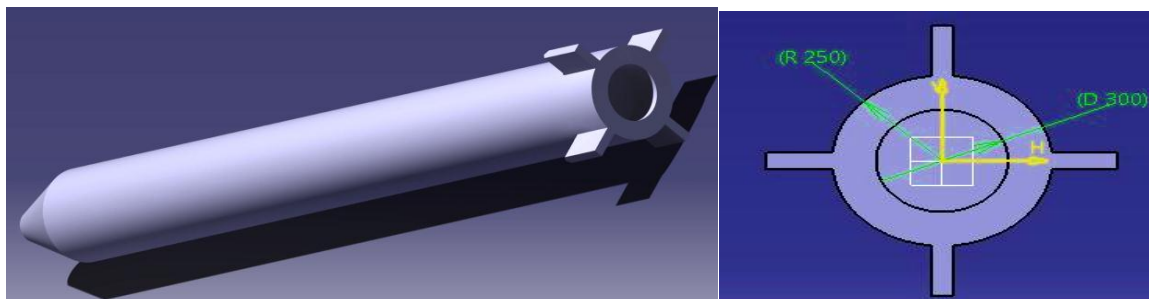


Fig. 4 Design with base cavity and dimensions of the cavity

4.4 Rocket Body with Fin Tapered at Trailing Edge

In this configuration, trailing edge of the fin is also tapered with the same parameters as fin tapered at the leading edge keeping all other dimensions of fin and body same as that of base model.

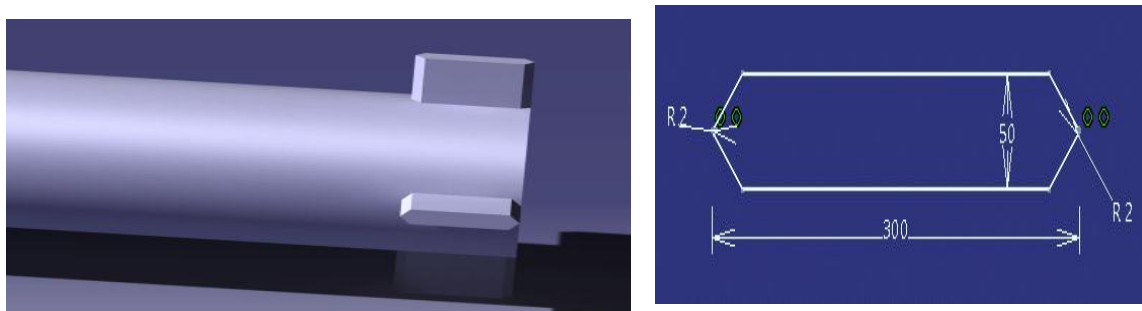


Fig. 5 Configuration with fin tapered at leading and trailing edge with the dimensions

4.5 Rocket Body with Fin Tapered Along Body Line

The fin is tapered along the body line from 25mm after leading edge to trailing edge so that trailing edge becomes sleeker, keeping all other dimensions of fin and body same as that of base model.

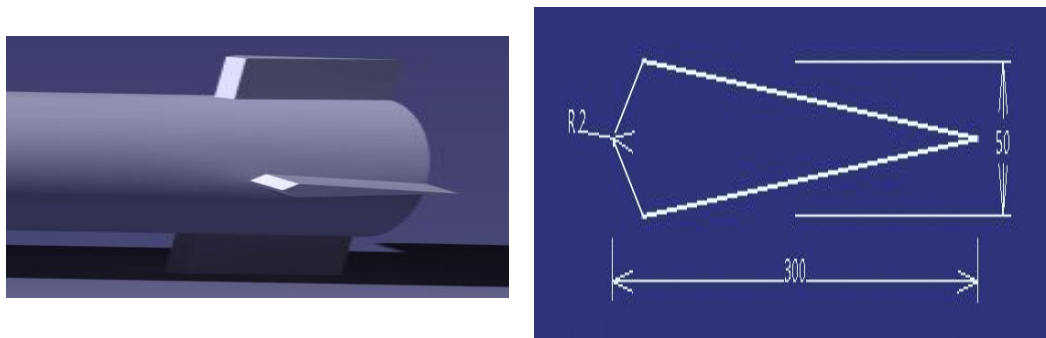


Fig. 6 Configuration with fin tapered along the body line with dimensions

Fin Configuration Considered:

4.6. Basic Fin

This fin model is used for 3 cases in this project which include basic configuration, boat tail and base cavity. Basic fin configuration is taken as a reference model, it is a simple geometry with tapered leading edge and blunt base as shown in the Fig. 7 and the dimensions are as of Table 4.

Table 4 Dimension of basic fin design

Fin semi span	150mm
Root chord	300mm
Thickness	50mm
Taper angle	45 degrees
Leading edge radius	2mm

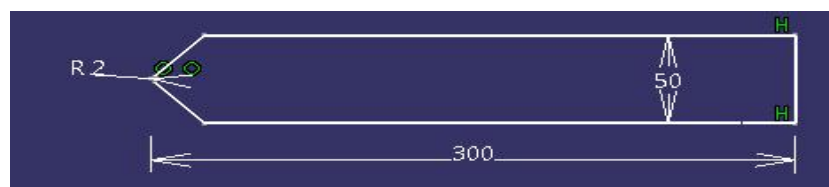


Fig. 7 Basic fin

4.7. Fin Tapered at Trailing Edge

Trailing edge of the fin is also tapered with the same parameters as fin tapered at the leading edge keeping all other dimensions of fin same as the basic fin (Fig.7). The fin design is given in Fig.8.

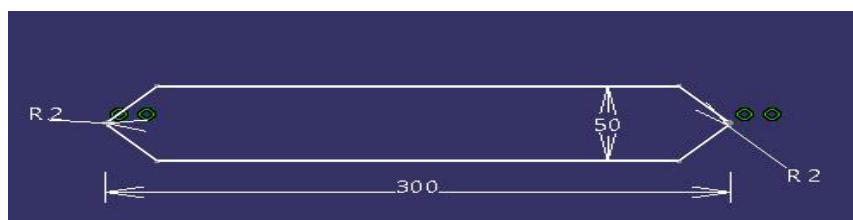


Fig. 8 Fin tapered at trailing edge

4.8 Fin Tapered Along Body Line

The fin is tapered along the body line from 25mm after leading edge to trailing edge so that trailing edge becomes sleeker, keeping all other dimensions of fin same as basic fin.

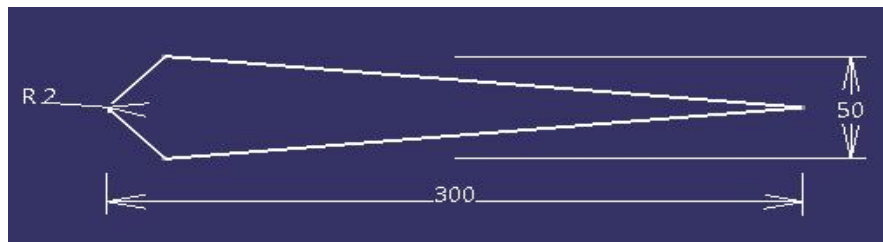


Fig. 9 Fin tapered along body line

It has a trailing taper angle of 5.2 degrees with root chord of 300mm.

4.9 Fin Tapered After 54%

Fin tapered after 54% is a type of which is tapered at leading edge and at 54% of length from its leading edge, keeping all other dimensions similar to basic fin.

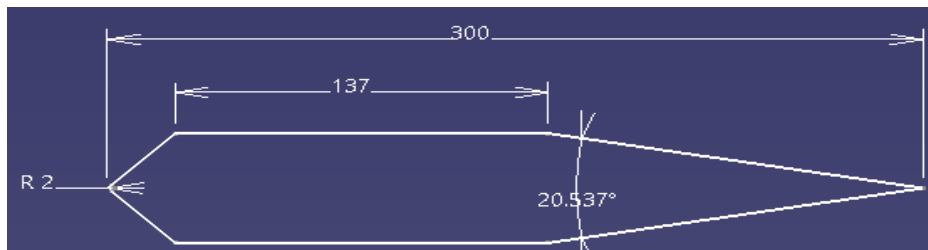


Fig. 10 Fin tapered after 54%

4.10. Fin Tapered After 75%

Fin tapered after 75% is a type of which is tapered at leading edge and at 75% of length from its leading edge, keeping all other dimensions similar to basic fin.

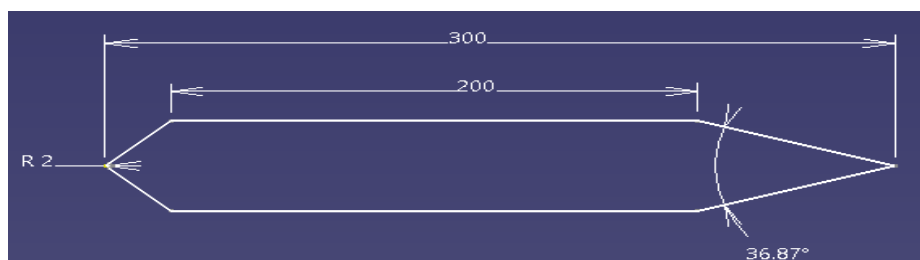


Fig. 11 Fin tapered after 75%

5. RESULTS AND DISCUSSIONS

5.1. Paras analysis

The above five configurations are analysed. The aerodynamic coefficients for four different Mach numbers in each case have been obtained through flow simulations in PARAS 3D software. The configurations are compared with the reference model that is the basic configuration.

5.1.1 C_A Comparison

The variation of C_A for Mach number 1.20 is shown below, the plot contains the C_A value of five configuration listed as case 1,2,3,6 and 7. From the plot, it is observed that the only change in C_A from basic configuration is at the base of each model where geometric changes have been made from basic configuration.

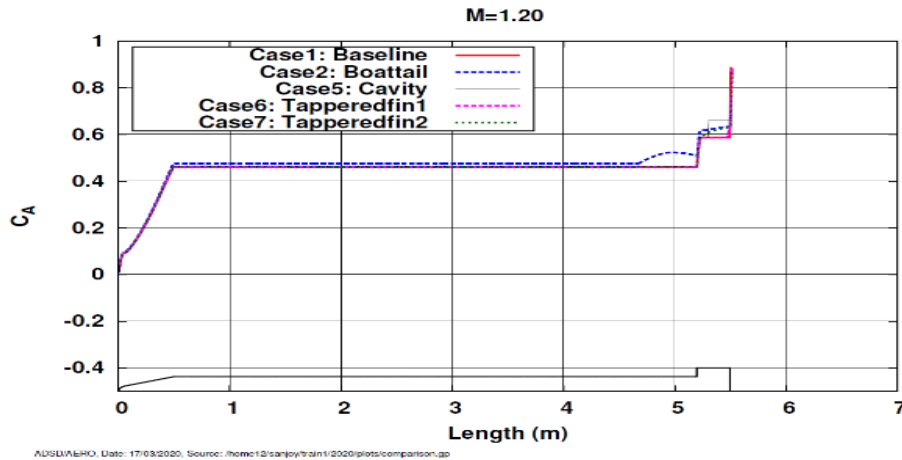


Fig. 12 C_A comparison plot of five different configuration for Mach number 1.20

The chart shown in Fig. 14 represents the comparison of final C_A of every case for four different Mach numbers. The final C_A for each case is shown in Table 5. From the bar graph shown in Fig. 14, it is observed that boat tail has minimum C_A at all Mach numbers with a drag reduction of average 25% in the boat-tail configuration in comparison with the reference model. Fin tapered along body line shows its effectiveness at higher Mach numbers. Both base cavity and fin tapered at trailing edge have less than 1% effect in the drag reduction. The figure 13 is the flow field diagram of boat-tailing with reference model at Mach 1.05, it is evident from the diagram that there is an increment in the base pressure due to the boat-tailing which contribute in the reduction of base drag.

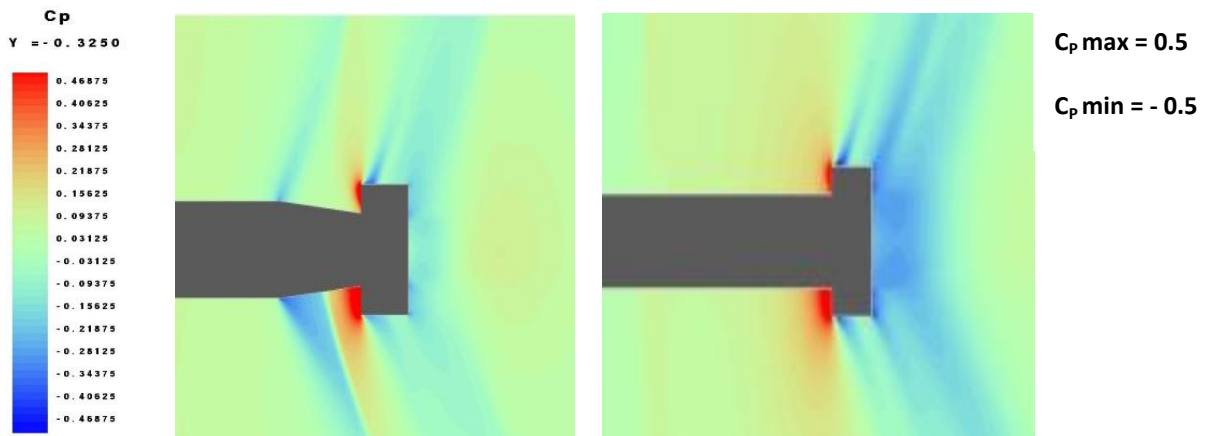


Fig. 13 Flow field diagram of boat tail along with reference model at Mach 1.05

Table 5 Comparison of final C_A values

Mach numbers	Base body	Boat tailing	Base cavity	Fin tapered at trailing edge	Fin tapered along body line
M=0.80	0.39	0.28	0.39	0.39	0.40
M=0.90	0.51	0.38	0.51	0.51	0.52
M=1.05	0.81	0.61	0.81	0.81	0.79
M=1.20	0.89	0.74	0.88	0.88	0.87

Table 6 Reduction of C_A compared to base body in percentage

Mach numbers	Base body	Boat tailing	Base cavity	Fin tapered at trailing edge
M=0.80	28	0	0	-2.5
M=0.90	25	0	0	-1.9
M=1.05	24	0	0	2.4
M=1.20	16	1.1	1.1	2.2

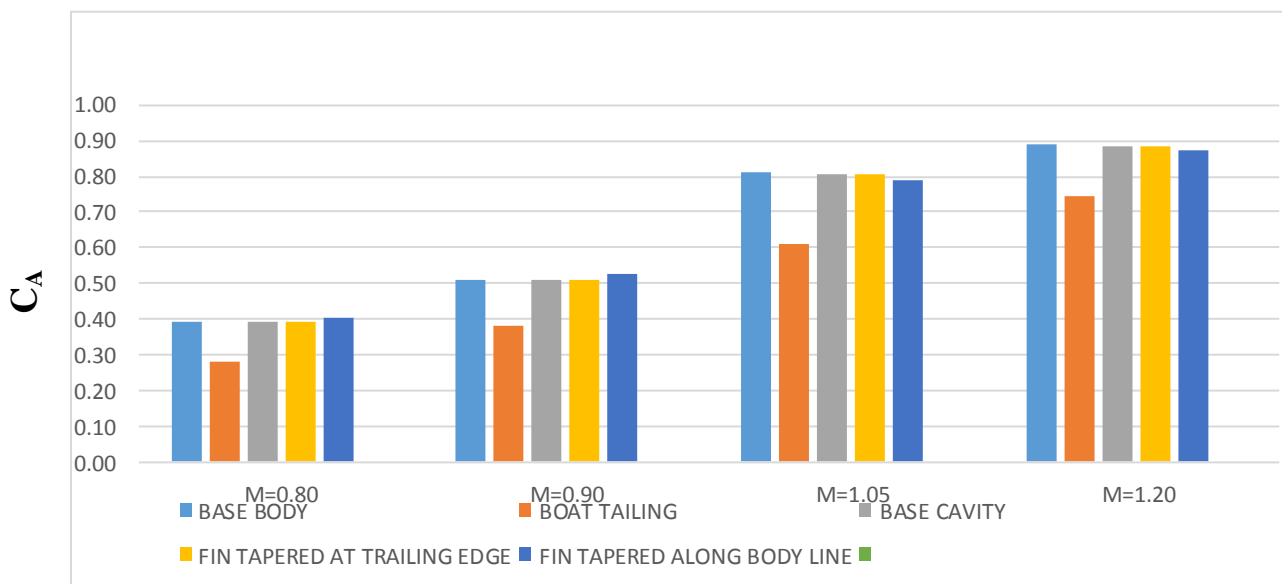


Fig. 14 Graphical representation of final C_A values for different configuration

5.1.2 C_N Comparison

The chart in Fig.15 shows the variation level of C_N for different Mach numbers for values shown in Table 6. From the comparison plot it is revealed that boat-tailing has significant reduction in C_N values when compared to other cases. From analysing the bar chart, it is found that the boat tailing has an average reduction of about 25% of C_N in each case.

Table 6 Comparison of final C_N values

Mach numbers	Base body	Boat tailing	Base cavity	Fin tapered at trailing edge	Fin tapered along body line
M=0.80	0.32	0.24	0.31	0.27	0.25
M=0.90	0.28	0.25	0.29	0.28	0.26
M=1.05	0.38	0.27	0.39	0.38	0.32
M=1.20	0.39	0.29	0.39	0.40	0.37

Table 7 Reduction of C_N compared to base body in percentage

Mach numbers	Base body	Boat tailing	Base cavity	Fin tapered at trailing edge
M=0.80	25	3	15	21
M=0.90	10	0	0	7
M=1.05	28	0	0	15
M=1.20	25	0	0	5

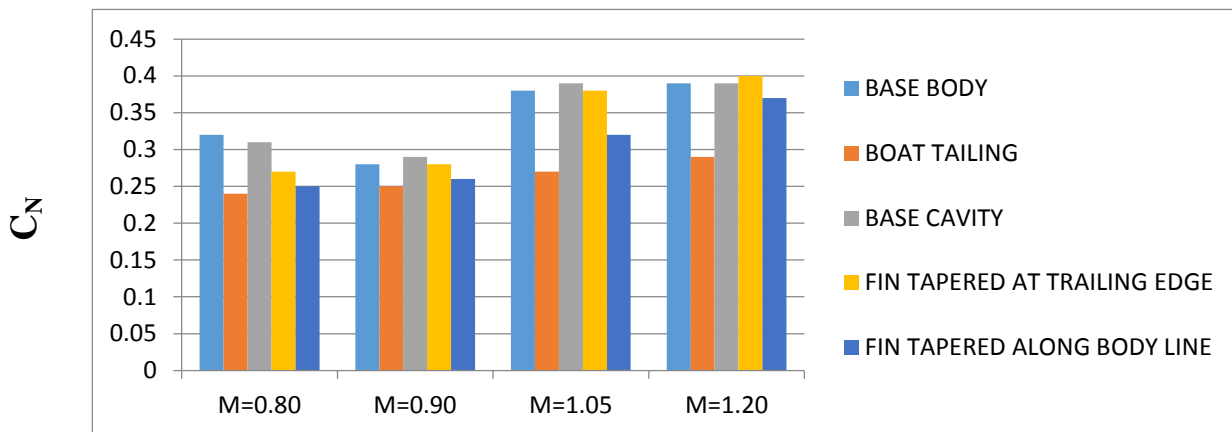


Fig.15 Graphical representation of final C_N values for each configuration for each Mach number

5.1.3 X_{CP} Comparison

The significance of distance of center of pressure (X_{CP}) is that it decides the stability of the vehicle and gives a dimensional value in the analysis. The length is measured in meters from the nose which is taken as the origin. X_{CP} values of five cases at Mach 0.8, 0.9, 1.05 and 1.20 are given in the Table 8.

$$X_{CP} = (C_{PM} / C_N) * \text{Reference length}$$

MACH NUMBERS	BASE BODY (m)	BOAT TAILING (m)	BASE CAVITY (m)	FIN TAPERED AT TRAILING EDGE (m)	FIN TAPERED ALONG BODY LINE (m)
M=0.80	2.44	2.56	3.01	2.57	2.50
M=0.90	2.78	2.54	2.89	2.71	2.57
M=1.05	3.19	2.37	3.25	3.19	2.84
M=1.20	3.23	2.55	3.20	3.24	3.10

For most of the Mach numbers, the X_{CP} for the boat-tailed case is closer to the nose. This is because of the reduced C_N at the base. Hence, boat-tailing may have an adverse effect on vehicle stability.

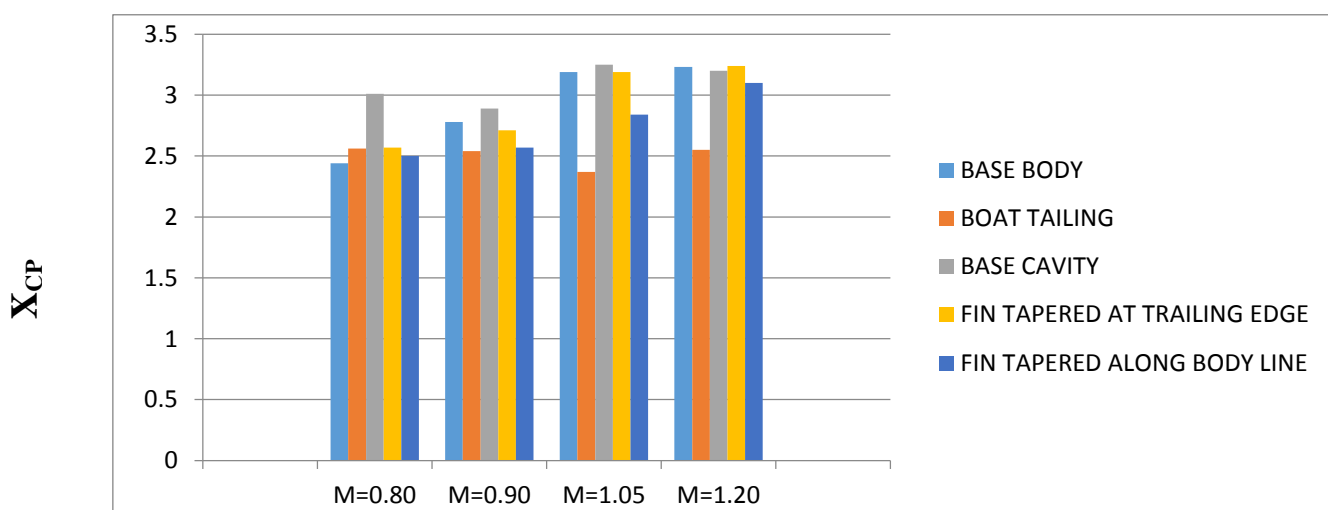


Fig. 16 Overall comparisons of X_{CP} for all cases and four Mach numbers

5.2 FIN ANALYSIS IN PARAS

In this analysis, three types of fins are used which includes basic fin, fin tapered at trailing edge and fin tapered along body line. Three dimensional fins with cruciform arrangement is used in this analysis. The results obtained are given below. In this analysis, the forces and moments on fins are isolated from the simulations over the complete vehicle. Separate simulation for fin alone was not conducted.

5.2.1 Fin C_A Comparison

Comparison of C_A of each case with different Mach number has been done to understand the drag associated with each model. For this analysis, overall C_A and C_A along body length have been plotted for each case. The Fig 17 shows the C_A plots along the length of fin for different Mach numbers.

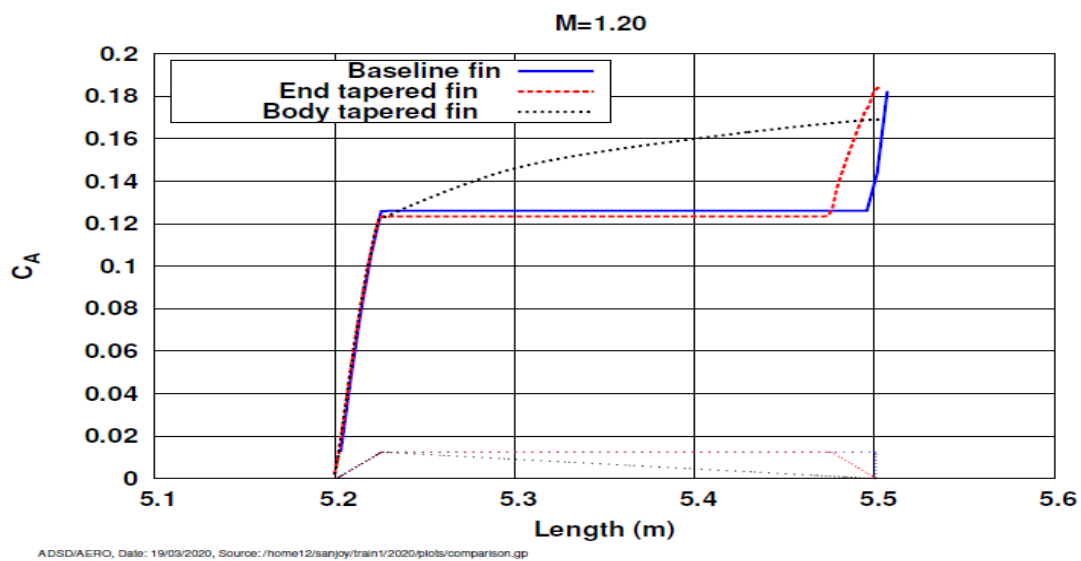


Fig. 17 Comparison plot of overall C_A values for three fins at Mach number 1.20.

From the C_A comparison along the body line, it is noticed that the variation of C_A along the leading edge is similar for each case due to the similarity in geometry., it is observable from fig 18 that the C_A value increases for lower Mach (0.80 and 0.90) and gradually decrease as the velocity increases (Mach 1.05 and 1.20) for fin tapered along body line. Hence it is more efficient at higher Mach numbers.

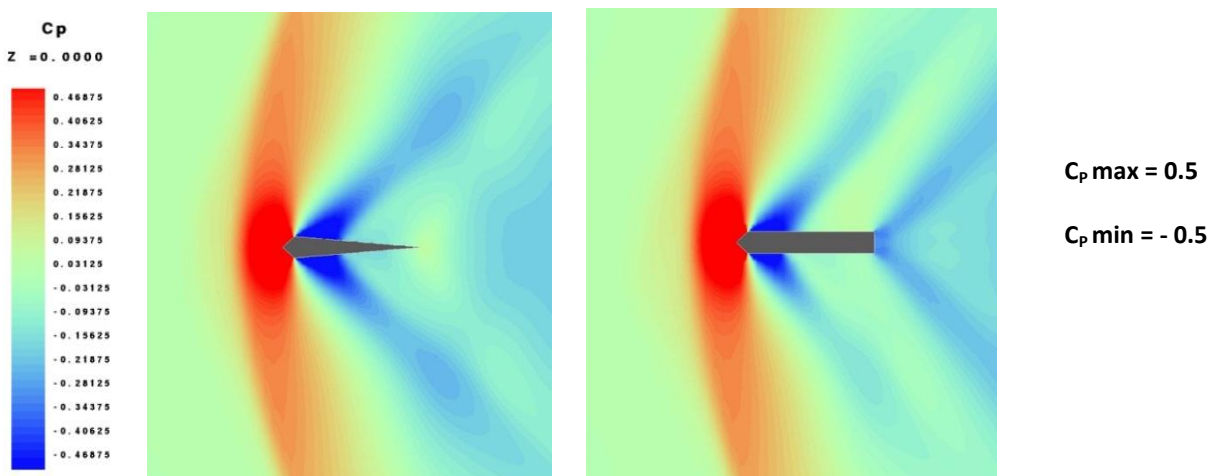


Fig. 18 Flow field diagram of boat tail along with reference model at Mach 1.20

Overall values of C_A for different cases for different Mach numbers has been plotted to understand the effectiveness of each fin model. The Fig 19 shows the bar graph of C_A . The same is given in Table 9.

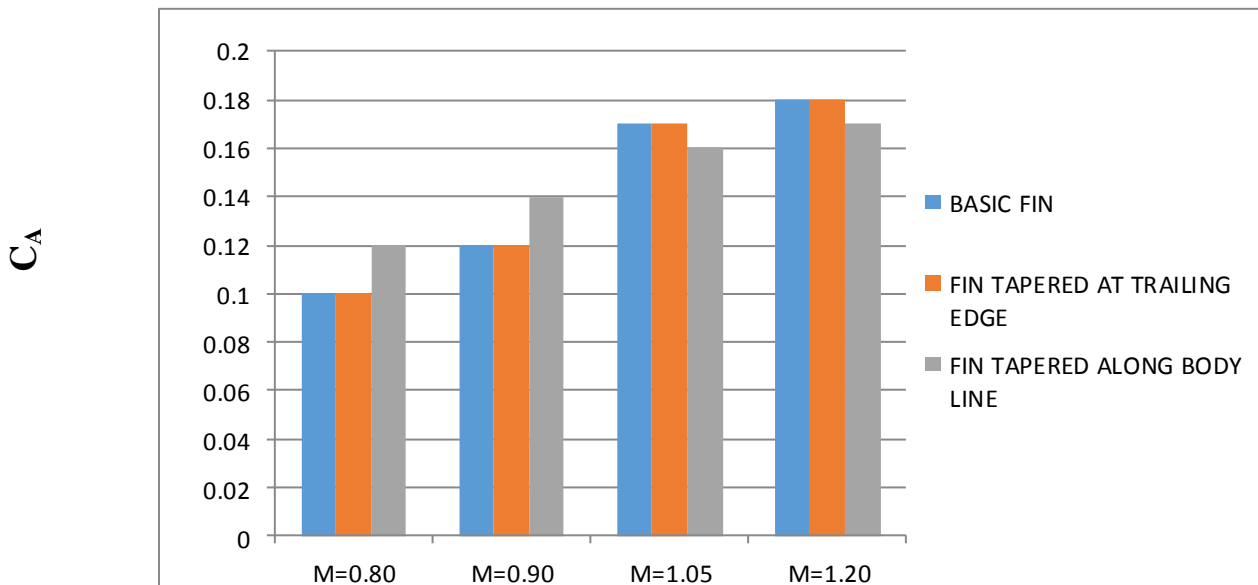


Fig.19 Overall C_A comparison

Table 9 Overall C_A values

MACH NUMBER	BASIC FIN	FIN TAPERED AT TRAILING EDGE	FIN TAPERED ALONG BODY LINE
M=0.80	0.10	0.10	0.12
M=0.90	0.12	0.12	0.14
M=1.05	0.17	0.17	0.16
M=1.20	0.18	0.18	0.17

From the above graph it is observed that basic fin model is effective at subsonic Mach numbers while fin tapered along body line is effective at supersonic Mach numbers.

5.2.2 Fin C_N Comparison

Overall values of C_N for different cases for different Mach numbers has been plotted to understand the effectiveness of each fin model. Fig 20 shows the bar graph of C_N for each Mach numbers compared among different cases. This data is also given in Table 10.

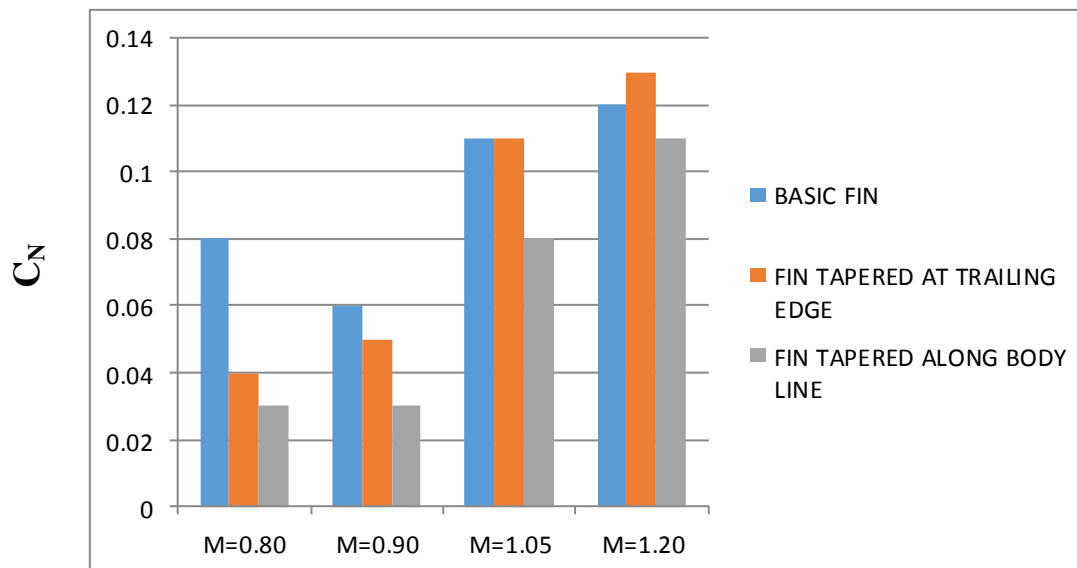


Fig. 20 Overall C_N comparison

Table 10 Overall C_N values

MACH NUMBER	BASIC FIN	FIN TAPERED AT TRAILING EDGE	FIN TAPERED ALONG BODY LINE
M=0.80	0.08	0.04	0.03
M=0.90	0.06	0.05	0.03
M=1.05	0.11	0.11	0.08
M=1.20	0.12	0.13	0.11

It is observed that the C_N values are highest for the basic fin and lowest for the fin tapered along the body line for all the Mach numbers. For Mach 1.20 the basic fin and fin tapered at the trailing edge has almost the same value, but for all other Mach numbers fin tapered at trailing edge has lower C_N value compared to the basic fin.

5.3 FIN ANALYSIS IN ANSYS

In this study five types of fins are used for flow simulation in ANSYS which includes basic fin, fin tapered at trailing edge, fin tapered along body line, fin tapered after 54%, fin tapered after 75%. CATIA V5 software is used to design the geometry and the flow field simulation of each case is conducted using ANSYS software. The domain for simulation is 6m x 6m cross section and meshing is done using element order line and element size 0.06 m with maximum layer of two. Quality of mesh is set as high with target skewness 0.90. Methods like edge sizing and face mapping are used to get finer meshing. The flow field studies of fin models are done for Mach numbers 0.80, 0.90, 1.05, 1.20 and 2. Flow simulation in ANSYS is a 2D analysis (of a single fin) while flow simulation in PARAS is done for a cruciform fin arrangement (3D geometry).

5.3.1 Fin C_A Comparison

The C_A value for different fin geometries at each Mach number is given in Table 11. Fig 22 shows the graphical comparison of different fins at each Mach number. From the bar graph, it is noticed that basic fin has less base drag at subsonic Mach numbers (i.e., 0.80 and 0.90) while fin tapered along body line has less drag at supersonic Mach numbers (i.e., 1.05, 1.20 and 2) as shown in figure 21. Both PARAS and ANSYS fin analysis yield the same result, that is basic fin is more effective at subsonic Mach numbers and fin tapered along body line is more effective at supersonic Mach numbers.

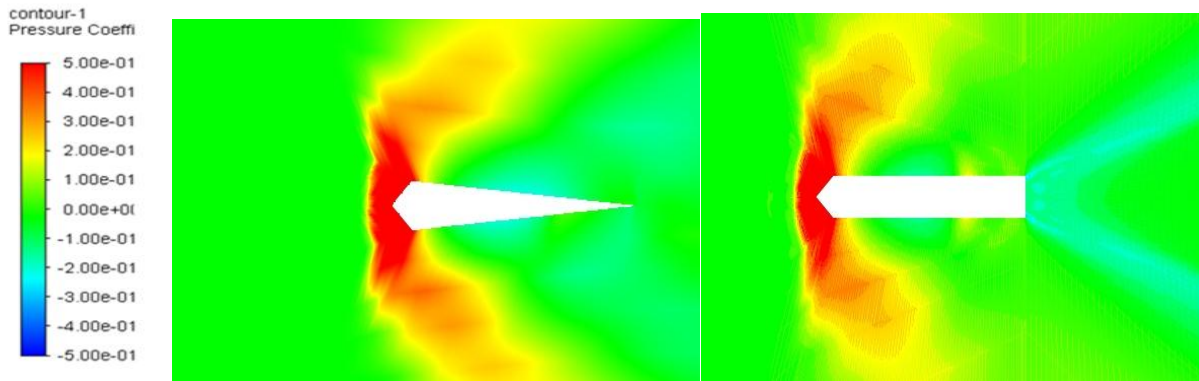


Fig. 21 Flow field diagram in ANSYS for tapered along bodyline fin with basic fin at Mach 2.0

*Reference length = 0.5 m Reference area = 0.19634 m²

Table 11 C_A values of various fin geometries at five different Mach numbers

Mach No.	Basic fin	Tapered trailing edge	Tapered along body	Tapered after 54% length	Tapered after 75% length
0.80	0.030	0.034	0.037	0.029	0.0518
0.90	0.039	0.044	0.048	0.055	0.054
1.05	0.045	0.051	0.045	0.049	0.051
1.20	0.041	0.045	0.039	0.043	0.044
2.00	0.029	0.030	0.028	0.029	0.031

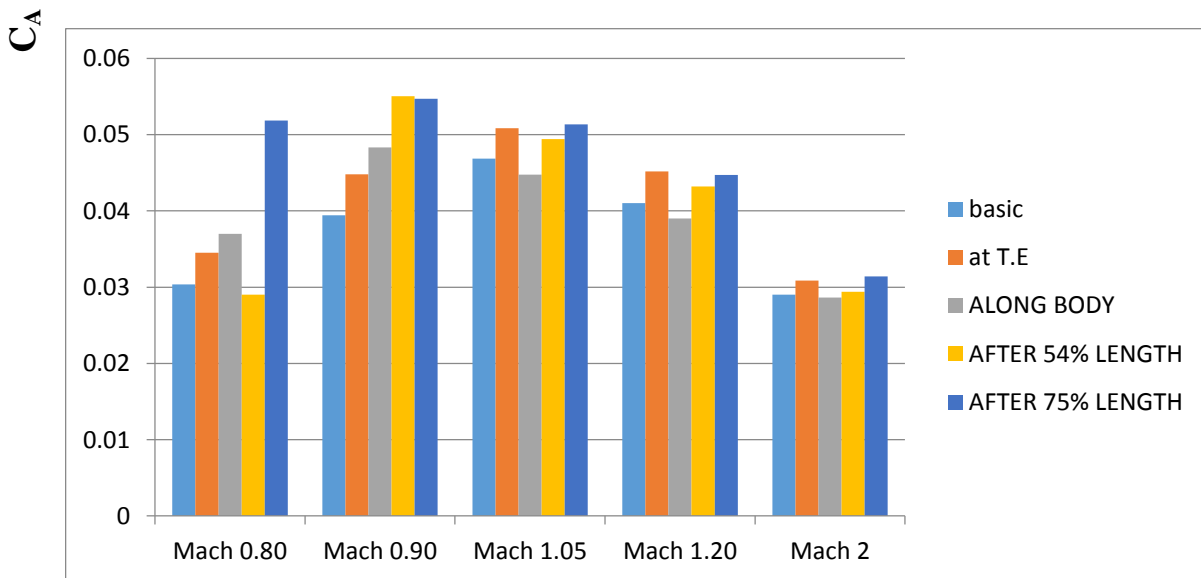


Fig. 22 Fin comparison chart

6. CONCLUSION

The objective of the project was to study and analyse some of the base drag reduction methods like aft body alteration and fin design alteration. Analysis of five different fins and 3 different base configurations are conducted using PARAS and ANSYS software. The aim of the analysis of these different configurations was to increase the base pressure, because base pressure is inversely proportional to the base drag. Using PARAS, five configurations are analysed; they are reference model, boat-tailed model, base cavity model, model with fin tapered at the trailing edge and model with fin

tapered along the body. All the configurations have less drag compared to the reference model. Among these configurations, boat tailed model show the least drag (25% less than reference model). Also, at higher Mach numbers, the model with fin tapered along the body shows less drag compared to the reference model but not low as the boat tailed model. Hence, boat tailing is the most suitable method for base drag reduction. Moreover, unlike base cavity, boat tailing is applicable for vehicles with or without jet.

Three different fin geometries (basic fin, fin tapered at trailing edge, and fin tapered along body line) have been analysed in PARAS 3D SOFTWARE at four different Mach numbers (0.80, 0.90, 1.05, and 1.20). The fin analysis on PARAS shows that basic fin is effective at subsonic Mach numbers (0.80 and 0.90) and fin tapered along body line is effective at supersonic Mach numbers (1.05 and 1.20).

ANSYS 2D analysis of five different fins is conducted at five different Mach numbers (0.80, 0.90, 1.05, 1.20 & 2.0). The five geometries considered are basic fin, fin tapered at trailing edge, fin tapered along the body, fin tapered after 54% length, fin tapered after 75% length. The analysis shows that the tapering has less effect on subsonic speeds. But the drag reduction is high when the speed becomes supersonic. Fin tapered along the body has the least drag at Mach numbers higher than one. By analysis, it is observed that the drag decreases as the tapering along the length is increased for higher speeds.

REFERENCES

1. Jan-Kaung Fu, Kangshan, Kaohsiung and Shen-Min Liangt: "Drag Reduction for Turbulent flow over a Projectile
2. P.R Viswanath:" Flow management techniques for base and after-body drag reduction".
3. S. A. Khan, Mohammed Asadullah and JafarSadhiq "Passive Control of Base Drag Employing Dimple in Subsonic Suddenly Expanded Flow".
4. M. A. Suliman, O. K. Mahmoud, M. A. Al-Sanabawy, O. E. AbdelHamid: "Computational Investigation of Bas Drag Reduction for a Projectile at Different Flight Regimes"
5. Aljallis, Elias,: "Experimental study of skin friction drag reduction on superhydrophobic flat plates in high Reynolds number boundary layer flow."
6. Y.K. Lee, H.D. Kim and S. Raghunathan: "A Study of Base Drag Optimization Using Mass Bleed"
7. VibhavDurgesh, Jonathan W. Naughton and Stephen A. Whitmore: "Experimental Investigation of Base-Drag Reduction via Boundary-Layer Modification"